Journal of Pain Research

Dovepress
open access to scientific and medical research

Open Access Full Text Article

ORIGINAL RESEARCH

# Partial sciatic nerve ligation leads to an upregulation of $Ni^{2+}$-resistant T-type $Ca^{2+}$ currents in capsaicin-responsive nociceptive dorsal root ganglion neurons



This article was published in the following Dove Medical Press journal:
*Journal of Pain Research*

Monika Jeub[1,2,*]
Omneya Taha[1,2,*]
Thoralf Opitz[2]
Ildiko Racz[3,4]
Julika Pitsch[5]
Albert Becker[5]
Heinz Beck[2]

[1]Department of Neurology, University of Bonn Medical Center, Bonn, Germany; [2]Department of Epileptology, University of Bonn Medical Center, Bonn, Germany; [3]Institute of Molecular Psychiatry, University of Bonn Medical Center, Bonn, Germany; [4]Department of Neurodegenerative Diseases and Gerontopsychiatry, University of Bonn Medical Center, Bonn, Germany; [5]Department of Neuropathology, University of Bonn Medical Center, Bonn, Germany

*These authors contributed equally to this work

**Background:** Neuropathic pain resulting from peripheral nerve lesions is a common medical condition, but current analgesics are often insufficient. The identification of key molecules involved in pathological pain processing is a prerequisite for the development of new analgesic drugs. Hyperexcitability of nociceptive DRG-neurons due to regulation of voltage-gated ion-channels is generally assumed to contribute strongly to neuropathic pain. There is increasing evidence, that T-type $Ca^{2+}$-currents and in particular the $Ca_v3.2$ T-type-channel isoform play an important role in neuropathic pain, but experimental results are contradicting.

**Purpose:** To clarify the role of T-type $Ca^{2+}$-channels and in particular the $Ca_v3.2$ T-type-channel isoform in neuropathic pain.

**Methods:** The effect of partial sciatic nerve ligation (PNL) on pain behavior and the properties of T-type-currents in nociceptive DRG-neurons was tested in wild-type and $Ca_v3.2$-deficient mice.

**Results:** In wild-type mice, PNL of the sciatic nerve caused neuropathic pain and an increase of T-type $Ca^{2+}$-currents in capsaicin-responsive neurons, while capsaicin-unresponsive neurons were unaffected. Pharmacological experiments revealed that this upregulation was due to an increase of a $Ni^{2+}$-resistant $Ca^{2+}$-current component, inconsistent with $Ca_v3.2$ up-regulation. Moreover, following PNL $Ca_v3.2$-deficient mice showed neuropathic pain behavior and an increase of T-Type $Ca^{2+}$-currents indistinguishable to that of PNL treated wild-type mice.

**Conclusion:** These data suggest that PNL induces an upregulation of T-Type $Ca^{2+}$-currents in capsaicin-responsive DRG-neurons mediated by an increase of a $Ni^{2+}$-insensitive current component (possibly $Ca_v3.1$ or $Ca_v3.3$). These findings provide relevance for the development of target specific analgesic drugs.

**Keywords:** T-type $Ca^{2+}$ channel, nociceptive DRG neuron, neuropathic pain, $Ca_v3.2$ knockout mice, partial sciatic nerve ligation

## Introduction

Neuropathic pain resulting from peripheral nerve lesions is characterized by abnormal sensory phenomena such as hyperalgesia (exaggerated pain response to a painful stimulus), allodynia (pain response to a normally not painful stimulus), or even spontaneous pain. Current therapies are often ineffective or limited by side effects. The elucidation of key molecules involved in pathological pain states may help in the development of new and improved analgesic drugs. The mechanisms leading to neuropathic pain involve complex pathophysiological changes of the peripheral and central nervous systems. On

Correspondence: Monika Jeub
Department of Epileptology, University of Bonn Medical Center, Sigmund-Freud-Str. 25, 53105 Bonn, Germany
Tel +49 228 287 15727
Email monika.jeub@ukbonn.de

submit your manuscript | www.dovepress.com
Dovepress
http://dx.doi.org/10.2147/JPR.S138708

the level of DRG neurons, neuropathic pain is associated with signs of hyperexcitability, such as reduced action potential threshold, increased action potential frequency, and ectopic discharges. T-type $Ca^{2+}$ channels play a fundamental role in promoting neuronal excitability by inducing low-threshold $Ca^{2+}$ spikes, burst firing, and post-hyperpolarization rebound action potentials.[1] As the $Ca_v3.2$ T-type $Ca^{2+}$channel isoform is expressed abundantly in nociceptive DRG neurons, interest has been focused on T-type channels as possible key candidates involved in normal and pathological pain signaling. Indeed, electrophysiological investigations of DRG neurons in different neuropathic pain models showed an increase of T-type currents, but other studies reported no change or a downregulation.[2–7] Analyses of mRNA levels in experimental pain models have also yielded contradicting results, with increased levels of $Ca_v3.2$ and $Ca_v3.3$ or no change for all three isoforms.[2,4,6] In vivo gene silencing of $Ca_v3.2$ by antisense oligonucleotides alleviated hyperalgesia in different neuropathic pain models and reversed the T-type current increase in a model of painful diabetic polyneuropathy.[5,8,9] Thus, a major role of $Ca_v3.2$ in neuropathic pain was suggested. However, pain tests of $Ca_v3.2$ knockout (KO) mice following spinal nerve ligation showed unaffected neuropathic pain behavior.[10] In the present study, we sought to clarify the following issues by using wild-type (WT) and $Ca_v3.2$ KO mice: Are T-type currents of nociceptive DRG neurons regulated in partial sciatic nerve ligation (PNL)-induced neuropathic pain? If so, is this due to altered currents of the $Ni^{2+}$-sensitive $Ca_v3.2$ subunit?

# Materials and methods

## Animals

Behavioral and electrophysiological experiments were carried out using $Ca_v3.2$ KO mice and WT littermates on a C57BL/6N background.[11] For all experiments 12–20-week-old female mice were used. The animals were housed in groups of six mice per cage under controlled illumination (light–dark cycle: 12:12 hours) and stable environmental conditions (temperature: 22°C±2°C; humidity: 55%±5%). All mice had free access to water and food pellets. Animals were housed in the cages for at least 1 week before the start of the experiments. Experiments were carried out in accordance with the Council Directive 2010/63 EU of the European Parliament, the Council of 22 September 2010 on the protection of animals used for scientific purposes, and the guidelines of the German Animal Protection Law and were approved by local authorities (Landesamt für Natur, Umwelt, und Verbraucherschutz NRW, AZ: 8.87–51.04.20.09.353). All efforts were made to minimize the number of animals used and their suffering.

## Behavioral assessment of neuropathic pain

Mice were first habituated to the experimental setup for >1 hour during 3 consecutive days. After the habituation period, baseline responses of both hindpaws were measured using the von Frey test. The von Frey filament test was conducted using a dynamic plantar esthesiometer (Ugo Basile Srl, Gemonio, Italy). The equipment consists of an electronically controlled mobile pressure actuator that exerts a continuously increasing force with a metal filament on the paw of tested animals. In the experimental setup, a maximal force of 15 g and a maximal ramp duration of 20 seconds were chosen. Paw withdrawal thresholds (PWTs) were automatically recorded as the withdrawal triggering force in grams. PWTs were calculated as the average of 3–5 consecutive trials with at least 3 minutes between each trial to avoid habituation. Measurements were performed 1 day before and 7 days after partial ligation of the sciatic nerve.

## Partial ligation of the sciatic nerve

Neuropathic pain was induced by partial ligation of the right sciatic nerve according to a method first described by Malmberg and Basbaum.[12] For this, mice were initially anesthetized with an oxygen/isoflurane mixture (2%–2.5% in 95% $O_2$), fixed on the surgery table, and kept under a constant stream of isoflurane (1.5%–2% in 95% $O_2$) to maintain anesthesia. The right sciatic nerve was exposed at midthigh level under aseptic condition. One-half to one-third of the nerve just proximal to the trifurcation was ligated with one tight ligation using a medical polypropylene thread (9–0). Finally, muscle and skin were strongly sutured with polypropylene threads (7–0; 5–0) and the animal was allowed to recover. Sham operation was performed in parallel in the control group mice by exposing the right sciatic nerve and then closing the wound without ligation. In all mice, the left leg was left untouched.

## Electrophysiology

Electrophysiological recordings were conducted 8-21 days after PNL or sham operation. Mice were deeply anesthetized with isoflurane and rapidly decapitated. $L_{4-5}$ dorsal root ganglia of ligated or sham-operated animals were collected in Neurobasal Medium A containing B27 supplement (Thermo Fisher Scientific, Waltham, MA, USA). Neurons were dissociated by addition of 0.125% crude collagenase general use type I (Sigma-Aldrich Co., St Louis, MO, USA) in an incubation chamber enriched with carbogen gas at 37°C for 1.5 hours. Following centrifugation and trituration, neurons

were resuspended in neurobasal medium and plated on poly-L-lysine (Sigma-Aldrich Co.) coated 35 mm diameter culture dishes and stored at 37°C in a humidified 5% $CO_2$ atmosphere. Cells were used for electrophysiological recordings within the culture dishes 1–8 hours after dissociation.

Small-size neurons (≤25 μm diameter), presumed to be nociceptive DRG neurons, were recorded in the whole-cell patch-clamp configuration at room temperature using an Axopatch 200B amplifier (Molecular Devices, Sunnyvale, CA, USA) controlled by pCLAMP8.2 software (Molecular Devices).[13] Patch pipettes with 3–4 MΩ resistance were fabricated from borosilicate glass capillaries (Science Products, Hofheim, Germany) using a P-97 Flaming/Brown Micropipette Puller (Sutter Instrument Company, Novato, CA, USA). One cell per culture dish was analyzed. Cells were not considered for analysis if they had high leakage currents (holding current ≥200 pA) or a series resistance greater than 12 MΩ. Passive membrane properties were measured in the voltage clamp mode by analyzing the current response to a 10 mV depolarizing voltage step for 135 ms from a –80 mV holding potential. The input resistance was determined according to Ohm's law from the steady-state current. Cell capacitance was determined by quantifying the charge (Q) required to fully charge the membrane. Q was measured as the total area under the current response to the aforementioned voltage step and cell capacitance $C_m$ was then calculated as Q/V, where V was the size of the voltage step. Series resistance $R_{series}$ was calculated as $\tau_{fast}/C_m$, where $\tau_{fast}$ was the fast time constant of the capacitative transient of the voltage step and was measured via a logarithmic biexponential fit.

Capacitance transients were canceled before each recording. Series resistance compensation (80%–90%) was applied to minimize voltage errors. Voltage errors were maximal at 1.5 mV. Data were filtered at 10 KHz and sampled at 20 KHz.

$Ca^{2+}$ channel currents were measured using $Ba^{2+}$ as charge carrier. All chemicals were obtained from Sigma-Aldrich Co. The extracellular solution used for T-type $Ca^{2+}$ current measurements contained (in mM): 152 tetraethylammonium chloride (TEA-Cl), 10 $BaCl_2$, and 10 4-(2-hydroxyethyl)-1-piperazineëthanesulfonic acid (HEPES) (305 mOsmol/L, pH =7.4 [TEA-OH]) (solution 1). To minimize contamination with high-voltage-activated (HVA) $Ca^{2+}$ currents, a fluoride ($F^-$)-based internal solution was used to facilitate run-down of HVA $Ca^{2+}$ currents. This solution contained (in mM): 135 TEA-OH, 10 EGTA, 40 HEPES, and 2 $MgCl_2$ (295 mOsmol/L, pH =7.2 [HF]) (solution 2).[3] Leakage currents were digitally subtracted using a P/6 or P/8 protocol. A liquid junction potential of +7 mV between intra- and extracellular solutions was calculated using Clampex 8.2 software, and membrane potentials were corrected accordingly. Drugs were prepared as stock solutions (100 mM $NiCl_2$ in $H_2O$, 100 mM $CdCl_2$ in $H_2O$, and 20 mM capsaicin in ethanol), freshly diluted in the bathing solution and delivered using a multichannel, gravity-driven system. Manually controlled valves were used to switch between.

As preliminary experiments showed that the external bathing solution used for $Ca^{2+}$ channel recordings leads to a complete and irreversible block of capsaicin-induced inward currents, measurements of capsaicin-evoked currents were performed just after obtaining the whole-cell configuration in a physiological extracellular solution containing the following (in mM): 150 NaCl, 5 KCl, 1 $CaCl_2$, 1 $MgCl_2$, and 10 HEPES (305 mOsmol/L, pH =7.4 [NaOH]) (solution 3). After measurement of the capsaicin-evoked current response, the bathing solution (solution 3) was switched to solution 1 to optimally isolate T-type $Ca^{2+}$ currents and $Ca^{2+}$ current measurements were performed. The intracellular solution was kept constant during the whole experiment. To verify recording of $Ca^{2+}$ channels, the cells were perfused at the end of the experiment with the external solution containing 50 μM $Ni^{2+}$ and 200 μM $Cd^{2+}$, which blocks all voltage gated $Ca^{2+}$ channels.

## Data analysis

Data analyses were done with Clampfit 9.2 software (Molecular Devices), Graphpad Prism (Graphpad Software, San Diego, CA, USA), and Excel 2003 on a Windows™-based PC system (Microsoft, Redmond, WA, USA). Data were tested for normality distribution using the Shapiro–Wilk test and for equal variances with an F-test. Analysis of electrophysiological data was done with the unpaired Student's *t*-test and if the *F*-test was not passed, Welch's correction was applied to the *t*-test. The distribution of capsaicin-sensitive and -insensitive cells was compared with the chi-squared test. Behavioral data were analyzed with the ANOVA test. For all tests, the significance level was set at $P \leq 0.05$. All data are presented as average ± standard error of the mean (SEM).

# Results

## PNL leads to neuropathic pain behavior in WT mice

WT mice were subjected to partial ligation of the right sciatic nerve or to a sham operation. The presence of PNL-induced neuropathic pain was tested by measuring the mechanical PWTs in the von Frey test (behavioral test for mechanical allodynia). All mice subjected to PNL displayed significantly decreased mechanical PWTs of the right side (ipsilateral,

ligated) 7 days after surgery compared to baseline values (ANOVA, $P \leq 0.001$, n=8) indicating the presence of PNL-induced neuropathic pain. In contrast, PWTs of the left side (contralateral, nonligated) or of sham-treated animals (n=6) were not affected (ANOVA, $P > 0.05$) (Figure 1).

## PNL of WT mice leads to an increase of T-type $Ca^{2+}$ currents in small, capsaicin-responsive DRG neurons

Small, presumably nociceptive neurons (diameter ≤25 µm) from $L_{4-5}$ DRGs of ligated and sham-treated WT mice were used for electrophysiological recordings as the sciatic nerve in mice originates from the spinal components L3 to L5.[14] Nociceptive neurons are inhomogeneous, and a classification according to their receptive properties is not possible after the dissociation process. We therefore classified cells according to their responsiveness to the TRPV1 receptor agonist capsaicin, which represents a commonly used binary classification scheme of isolated nociceptive DRG neurons.[15] TRPV1 is a polymodal nonselective cation channel that is activated by harmful heat, extracellular protons, and vanilloid compounds and is an important selective marker of nociceptive function.[16–18] In vivo polymodal heat and at least half of the mechanoheat nociceptive fibers display capsaicin sensitivity, whereas high-threshold mechanosensitive, mechanocold, chemosensitive, and some silent nociceptive fibers are capsaicin insensitive.[15] The percentage of cells responding with an inward current to application of 1 µM capsaicin (sham: 61%, PNL: 73%; chi-squared test, $P > 0.05$) (Figure 2Aa,b) as well as the magnitude of the capsaicin-induced current (capsaicin-sensitive cells: sham: 2.648 nA, PNL: 2.904 nA; unpaired *t*-test with Welch's correction, $P > 0.05$) (Figure 2Ac) was not significantly different between PNL and sham mice. To analyze the effect of PNL on T-type voltage-gated $Ca^{2+}$ currents, cells were held at –100 mV and total $Ca^{2+}$ currents were recorded via a standard pulse protocol with voltage steps from –70 mV to +10 mV (10 mV increments, 250 ms duration). The total $Ca^{2+}$ current of nociceptive DRG neurons consists of two main components: T-type $Ca^{2+}$ currents, which activate with small membrane depolarization and display fast and almost complete inactivation, and HVA $Ca^{2+}$ currents, which activate at more depolarized potentials and have very slow inactivation (sustained current). Figure 2B shows a representative family of total $Ca^{2+}$ currents in a small, capsaicin-responsive DRG neuron ($cap^+$ cell) from a sham- and PNL-treated animal, respectively. The T-type $Ca^{2+}$ current was isolated by subtracting the sustained current (HVA current) at the end of the depolarizing pulse from the peak current response. Average current–voltage curves were constructed, and a significant increase of the T-type $Ca^{2+}$ current in capsaicin-responsive cells from PNL mice was seen at negative test potentials, where T-type currents are most prominent (Figure 2C). To quantify the T-type $Ca^{2+}$ current, the peak current was calculated at –30 mV (peak of T-type current). There was a significant increase of the peak T-type current of $cap^+$ cells from PNL mice compared to $cap^+$ cells from sham mice (WT sham: n=13, wt PNL: n=20; unpaired *t*-test with Welch's correction, $P \leq 0.001$) (Figure 2Da), whereas there were no significant changes for $cap^-$ cells (WT sham: n=13, WT PNL: n=9; unpaired *t*-test with Welch's correction, $P > 0.05$) (Figure 2Db). To exclude a relevant contamination of these analyses with residual slowly inactivating HVA currents, T-type currents were isolated in a second way using a pre-pulse protocol based on the more hyperpolarized steady-state inactivation characteristics of T-type currents compared to HVA currents (Figure 2E). Similarly, we found a significant increase of the T-type peak current in $cap^+$

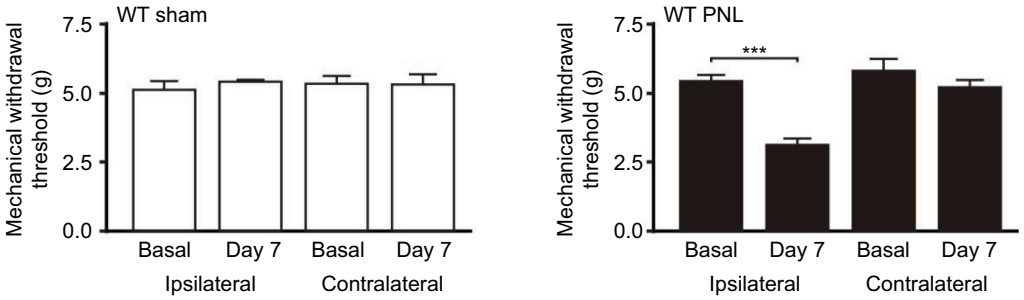


**Figure 1** PNL WT mice display neuropathic pain behavior 7 days after surgery.
**Notes:** Mechanical allodynia (von Frey test) was used as outcome measure of neuropathic pain. Mechanical paw withdrawal thresholds of the ipsilateral and contralateral hindpaw were tested before and 7 days after PNL or sham surgery of the right sciatic nerve. PNL mice displayed significantly reduced paw withdrawal thresholds of the ligated (right) side 7 days after surgery, whereas paw withdrawal thresholds of the unligated (left) side or of sham-operated animals were not affected; ***P≤0.001.
**Abbreviations:** PNL, partial sciatic nerve ligation; WT, wild type.

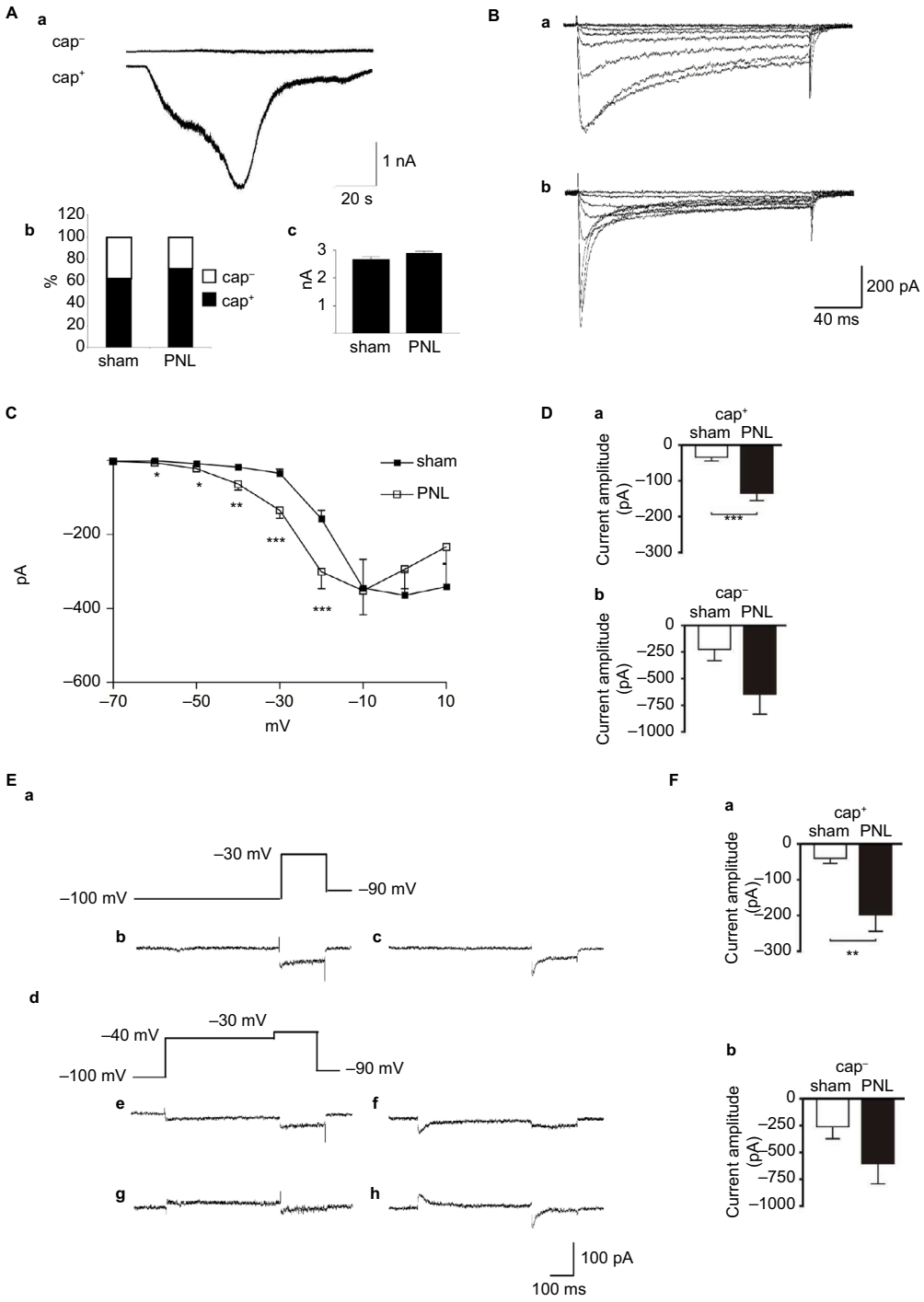


**Figure 2** PNL of WT mice leads to an increase of T-type $Ca^{2+}$ currents in small, capsaicin-responsive DRG neurons.

**Notes: (A)** Representative capsaicin currents of a capsaicin-insensitive (upper trace) and a capsaicin-sensitive (lower trace) small DRG neuron (**a**). Distribution of capsaicin-insensitive and capsaicin-sensitive cells in sham and PNL WT mice (**b**). Amplitude of the capsaicin current in capsaicin-sensitive cells of sham and PNL WT mice (**c**). (**B**) Total $Ca^{2+}$ currents of a representative $cap^+$ WT sham (**a**) and a $cap^+$ WT PNL cell (**b**) elicited from a holding potential of –100 mV by voltage steps ranging from –70 mV to 10 mV in 10 mV increments. Both T-type and HVA currents are present in both traces. **C**) Average current–voltage curves from experiments depicted in B. To isolate the T-type current, the amplitude of the inward $Ca^{2+}$ current was measured at each potential from the end of the pulse to its peak. PNL led to a significant increase of the T-type $Ca^{2+}$ current in $cap^+$ cells seen at negative test potentials, where T-type currents are most prominent. No significant changes were seen for $cap^-$ cells (current voltage–curve not shown). (**D**) Histogram showing average T-type $Ca^{2+}$ current amplitudes at –30 mV (peak of T-type current). Average peak current amplitudes were significantly increased in $cap^+$ cells following PNL (**a**), whereas there was no significant change for $cap^-$ WT PNL cells compared to $cap^-$ WT sham cells (**b**). (**E**) To quantify the T-type $Ca^{2+}$ current more exactly, cells were held at –100 mV and total $Ca^{2+}$ currents were evoked by a 200 ms depolarizing voltage step to –30 mV (**a**). Representative current traces of a $cap^+$ WT sham (**b**) and a $cap^+$ WT PNL cell (**c**). The HVA current component was separated by inactivating the T-type current via a preconditioning pre-pulse to –40 mV (**d**). Representative current traces of a $cap^+$ WT sham (**e**) and a $cap^+$ WT PNL cell (**f**). The T-type current was then obtained by digitally subtracting the HVA current component from the total $Ca^{2+}$ current. Representative current examples of a $cap^+$ WT sham (**g**) and a $cap^+$ WT PNL cell (**h**). (**F**) Average peak T-type currents were significantly increased in $cap^+$ WT PNL cells compared to $cap^+$ WT sham cells (**a**), whereas there was no significant difference for $cap^-$ cells (**b**). **P*≤0.05, ***P*≤0.01, ****P*≤0.001.

**Abbreviations:** DRG, dorsal root ganglion; HVA, high voltage activated; PNL, partial sciatic nerve ligation; WT, wild type.

PNL cells compared to cap$^+$ sham cells (unpaired *t*-test with Welch's correction, wt sham: n=6, wt PNL: n=16, $P \leq 0.01$) and no changes for cap$^-$ cells (WT sham: n=9, WT PNL: n=5; unpaired *t*-test with Welch's correction, $P > 0.05$) (Figure 2Fa, b). Differences in the T-type current amplitude of cap$^+$ cells were not explained by differences in passive membrane properties between sham and PNL mice (capacity, wt sham cap$^+$: 16.86±1.60 pF, wt PNL cap$^+$: 16.09±1.13 pF, wt sham cap$^-$: 16.62±2.58 pF, wt PNL cap$^-$: 13.43±0.87 pF; input resistance, wt sham cap$^+$: 675.07±85.11 MΩ; wt PNL cap$^+$: 822.70±115.89 MΩ, wt sham cap$^-$: 505.99±66.83 MΩ; wt PNL cap$^-$: 636.43±93.06 MΩ; unpaired *t*-test $P > 0.05$ for each parameter, data not shown).

To test whether the increased T-type current in cap$^+$ PNL cells is mediated by $Ca_v3.2$, we analyzed its sensitivity to $Ni^{2+}$. Only $Ca_v3.2$ channels are highly $Ni^{2+}$-sensitive ($IC_{50}$ ~10 µM), while $Ca_v3.1$ and $Ca_v3.3$ are 20-fold less sensitive allowing the discrimination of the total T-type current into $Ca_v3.2$ ($Ni^{2+}$-sensitive) and $Ca_v3.1$/$Ca_v3.3$ ($Ni^{2+}$-resistant).[19] T-type currents of cap$^+$ and cap$^-$ cells were measured with the same standard voltage protocol as described before. Application of 50 µM $Ni^{2+}$ led to the separation of the $Ni^{2+}$-resistant T-type component. The $Ni^{2+}$-sensitive component was derived by digitally subtracting the $Ni^{2+}$-resistant component from the total current (Figure 3A). $Ni^{2+}$ blocked 74% of the T-type current of sham cells and 69% of PNL cells, revealing the main T-type $Ca^{2+}$ current component of cap$^+$ DRG neurons to be $Ni^{2+}$- sensitive. However, comparing the $Ni^{2+}$-sensitive and $Ni^{2+}$-resistant current components between the experimental groups showed a significant increase of the $Ni^{2+}$-resistant current component after PNL (wt sham: n=10, wt PNL: n=14; unpaired *t*-test with Welch's correction, $P \leq 0.05$), whereas the $Ni^{2+}$-sensitive component was unchanged (wt sham: n=10, wt PNL: n=13; unpaired *t*-test with Welch's correction $P > 0.05$) (Figure 3B).

## $Ca_v3.2$ KO mice display unaltered neuropathic pain behavior after PNL

So far, these data reveal that PNL induces an upregulation of T-type $Ca^{2+}$ currents in small cap$^+$ DRG neurons and suggest that this increase is not due to the predominant $Ni^{2+}$-sensitive isoform $Ca_v3.2$, but is rather mediated by a $Ni^{2+}$-insensitive current. This is in contrast to some previous studies suggesting a role of the $Ni^{2+}$-sensitive T-type $Ca^{2+}$ isoform $Ca_v3.2$ in contributing to neuropathic pain.[8,9] To determine the role of $Ca_v3.2$ in PNL-induced neuropathic pain, behavioral experiments were performed in PNL and sham-operated $Ca_v3.2$ KO mice. PNL of the right sciatic nerve of $Ca_v3.2$ KO mice induced significantly reduced mechanical withdrawal thresholds in the von Frey test, revealing the presence of mechanical allodynia as correlate of neuropathic pain (n=8, $P \leq 0.001$, ANOVA). Mechanical withdrawal responses of the contralateral left hind paw and of sham-operated $Ca_v3.2$ KO mice were unaffected (n=7) ($P > 0.05$) (Figure 4). In addition, mechanical thresholds of ligated $Ca_v3.2$ KO mice were reduced to the same amount as in PNL WT mice indicating that $Ca_v3.2$ KO mice display identical neuropathic pain behavior as WT mice (WT PNL: 3.116 g, n=8, $Ca_v3.2$ KO PNL: 3.125 g, n=8; ANOVA, $P > 0.05$).

## PNL leads to an increase of T-type currents in capsaicin-responsive small DRG neurons of $Ca_v3.2$ KO mice

To further determine the role of the $Ca_v3.2$ subunit in PNL-induced neuropathic pain, $Ca^{2+}$ current recordings were performed in small DRG neurons of PNL and sham-operated $Ca_v3.2$ KO mice. The percentage of capsaicin-positive cells (sham: 75%, PNL: 69%; chi-squared test, $P > 0.05$) and the capsaicin current amplitude of capsaicin-sensitive cells was not different between groups (capsaicin-sensitive cells: sham (n=7): 2.466 nA, PNL (n=19): 3.065 nA; unpaired *t*-test with Welch's correction, $P > 0.05$) (Figure 5Aa, b). The T-type current of capsaicin-sensitive cells was quantified as described earlier. The T-type $Ca^{2+}$ current amplitude was small in sham-operated $Ca_v3.2$ KO mice, confirming that $Ca_v3.2$ is the predominant T-type channel isoform (Figure 5B, C). Comparing T-type currents of PNL and sham-operated $Ca_v3.2$ KO mice revealed a significant upregulation of the T-type-current in cap$^+$ DRG cells after PNL (Figure 5D shows standard pulse protocol, KO sham: n=12, KO PNL: n=11; unpaired *t*-test with Welch's correction $P \leq 0.01$; Figures 5E and F show preconditioning pulse, KO sham: n=6 and KO PNL: n=11; unpaired *t*-test with Welch's correction, $P \leq 0.05$). No changes in the T-type current peak amplitude were found for cap$^-$ neurons (KO sham: n=7, KO PNL: n=4; unpaired *t*-test with Welch's correction, $P > 0.05$ for both protocols) (Figure 5D, F). The amount of the increased T-type current in cap$^+$ cells of $Ca_v3.2$ KO mice was identical to that of cap$^+$ cells of WT mice following PNL (standard protocol at –30 mV, cap$^+$ PNL WT: 134.35±20.7 pA, n=20, cap$^+$ PNL $Ca_v3.2$ KO: 137.77±43.59 pA, n=11). Furthermore, analysis of the steady-state voltage dependence of activation and inactivation as well as of the time-dependent activation (10%–90% rise time) and time-dependent inactivation (time-dependent inactivation time constant) revealed identical properties of cap$^+$ PNL cells of WT and $Ca_v3.2$ KO mice (Figure 6).

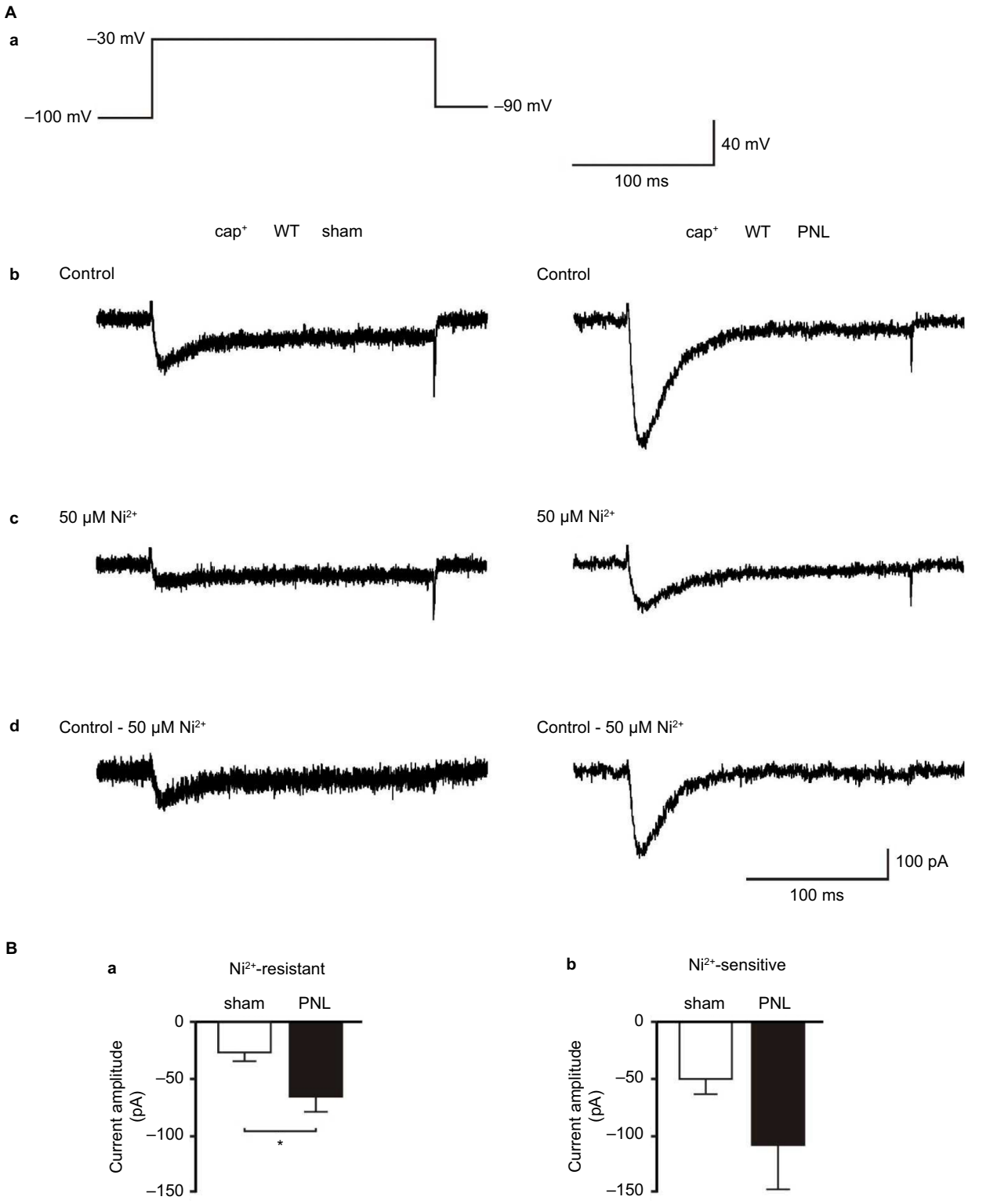


**Figure 3** The increase of the T-type-current in cap$^+$ WT cells following PNL is due to an increase of the $Ni^{2+}$-resistant current component.

**Notes: (A)** Total $Ca^{2+}$ currents were elicited via a standard voltage protocol and the peak T-type $Ca^{2+}$ current was quantified at –30 mV by subtracting the sustained current at the end of the depolarizing pulse from the peak current response (**a**). (**b**) Representative current traces of a cap$^+$ WT sham (left) and a cap$^+$ WT PNL cell (right). (**c**) Application of 50 µM $Ni^{2+}$ allowed the separation of a $Ni^{2+}$-resistant current component (left: cap$^+$ WT sham, right: cap$^+$ WT PNL). (**d**) The $Ni^{2+}$-sensitive current component was obtained by digitally subtracting the $Ni^{2+}$-resistant component from the total $Ca^{2+}$ current (left: cap$^+$ WT sham, right: cap$^+$ WT PNL). (**B**) Average peak current of the $Ni^{2+}$-resistant current (**a**) and the $Ni^{2+}$-sensitive current (**b**), *$P \leq 0.05$.

**Abbreviations:** PNL, partial sciatic nerve ligation; WT, wild type.

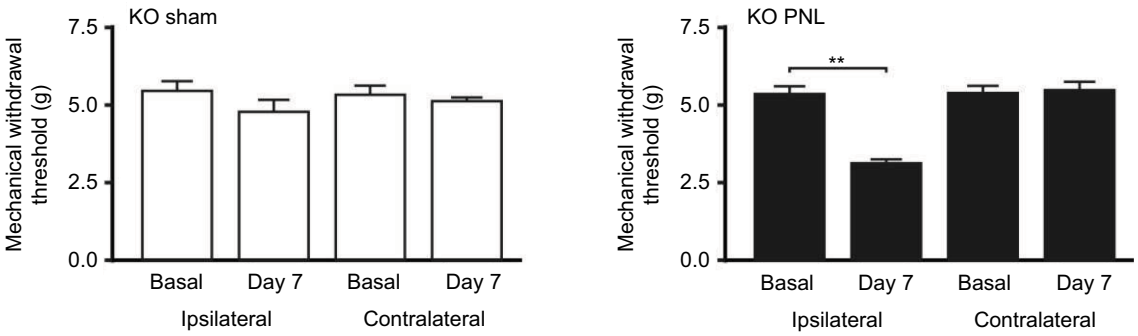


**Figure 4** $Ca_v3.2$ KO mice display unaltered neuropathic pain behavior following PNL of the sciatic nerve.
**Notes:** Right panel: PWTs of $Ca_v3.2$ KO mice before (day 0) and 7 days after PNL of the right sciatic nerve. PWTs of the right side (ipsilateral, ligated) were significantly reduced 7 days after PNL, whereas PWTs of the left side (contralateral, not ligated) were unchanged. Left panel: sham treatment of $Ca_v3.2$ KO mice did not affect PWTs, $^{**}P \leq 0.01$).
**Abbreviations:** KO, knockout; PNL, partial sciatic nerve ligation; PWTs, paw withdrawal thresholds.

A comparison of the $Ni^{2+}$-sensitive and $Ni^{2+}$-resistant T-type current components of cap$^+$ cells between sham-operated and PNL $Ca_v3.2$ KO mice showed a significant increase of the $Ni^{2+}$-resistant current component after PNL ($Ca_v3.2$ KO sham: n=9, $Ca_v3.2$ KO PNL: n=8, unpaired *t*-test with Welch's correction, $P \leq 0.05$), whereas there was no difference in the $Ni^{2+}$-sensitive current component ($Ca_v3.2$ KO sham: n=9, $Ca_v3.2$ KO PNL: n=8, $P > 0.05$) (Figure 7). There were no differences in the passive membrane properties between sham and PNL mice, which could explain the increase of the T-type current amplitude of cap$^+$ cells in PNL KO mice (capacity, $Ca_v3.2$ KO sham cap$^+$: 16.63 ±2.01 pF, $Ca_v3.2$ KO PNL cap$^+$: 14.84 ± 1.18 pF, $Ca_v3.2$ KO sham cap$^-$: 17.35±3.35 pF, $Ca_v3.2$ KO PNL cap$^-$: 14.09±1.52 pF; input resistance, $Ca_v3.2$ KO sham cap$^+$: 939.53±319.82 MΩ, $Ca_v3.2$ KO PNL cap$^+$: 696.08±75.70 MΩ, $Ca_v3.2$ KO sham cap$^-$: 1,006.37±462.98 MΩ, $Ca_v3.2$ KO PNL cap$^-$: 610.53±237.24 MΩ; unpaired *t*-test, $P > 0.05$ for each parameter). These data confirm that the upregulation of the T-type $Ca^{2+}$ current in nociceptive cap$^+$ DRG neurons after PNL is not mediated by $Ca_v3.2$.

## Discussion

In this study, we demonstrate that neuropathic pain induced by PNL of the sciatic nerve is associated with an upregulation of T-type $Ca^{2+}$ currents in small, nociceptive, capsaicin-responsive DRG neurons, whereas capsaicin-insensitive small DRG neurons are unaffected. Our pharmacological results in conjunction with experiments using $Ca_v3.2$ KO mice reveal that this is not due to a regulation of the predominant $Ca_v3.2$ T-type $Ca^{2+}$ channel isoform, but by an increase of a $Ni^{2+}$-resistant current.

Although recent reports have described an increase of T-type $Ca^{2+}$ currents in small and medium DRG neurons in different neuropathic pain models, earlier studies reported contradicting results showing no changes in small and medium DRG neurons or even a loss of T-type $Ca^{2+}$ currents in medium-sized DRG neurons.[3,7,20] These discrepancies cannot be explained only by differences in the animal model or species applied, as Hogan and McCallum used the identical model as Jagodic (chronic construction injury model of the sciatic nerve in the rat). We hypothesized that these differences might also be due to the heterogeneity of cells used in these studies, as small- and medium-sized DRG neurons are inhomogeneous groups of cells differing in their electrophysiological properties and in their responsiveness to sensory stimuli. To account for this, we focused only on small (diameter ≤25 µm) DRG neurons, as many functional studies have confirmed that the vast majority of them represent the cell bodies of nociceptive C-fibers, whereas the group of medium-sized DRG neurons comprise a mixture of both nociceptive and non-nociceptive cells. However, small DRG neurons are also diverse, and classification according to their sensory receptive properties is not possible after the dissociation process.[15,21] We therefore additionally subdivided small DRG neurons according to their responsiveness to the TRPV-1 agonist capsaicin, a commonly used pharmacological classification scheme of isolated nociceptive neurons.[15] The capsaicin sensitive represent mainly the cell bodies of not only polymodal nociceptive C-fibers, but also of C-heat and C-mechano-heat fibers.[15] However, as up to six functional subtypes of nociceptive C-fibers have been described in vivo, we cannot exclude an additional alteration of T-type $Ca^{2+}$ currents in single subgroups of capsaicin-negative cells or conclude that single subgroups of capsaicin-responsive cells are not affected.[15]

T-type currents have a key function in neuronal membrane oscillations and in generating action potentials as well as

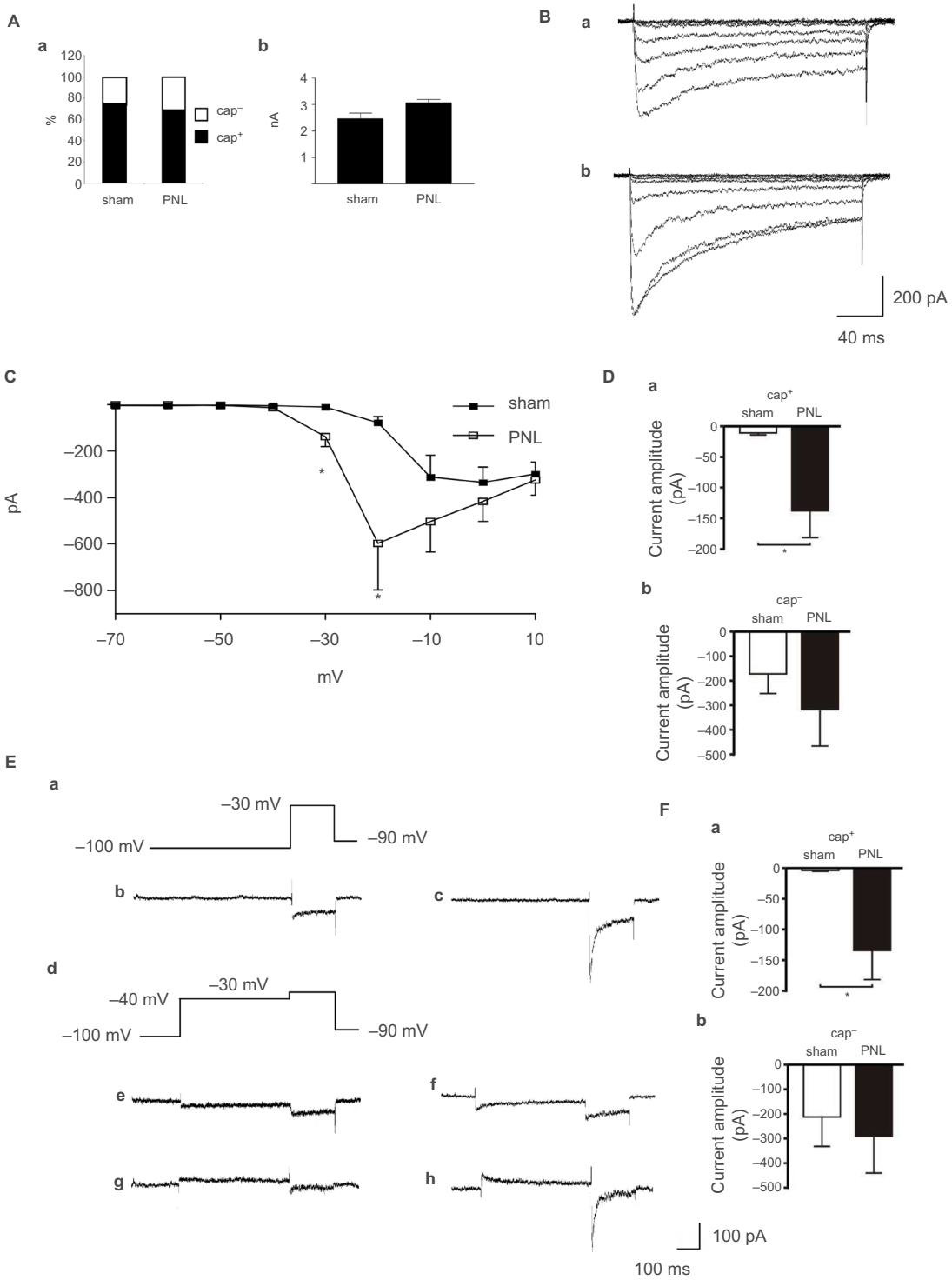


**Figure 5** The T-type $Ca^{2+}$ current is upregulated in small, capsaicin-responsive DRG neurons of $Ca_v3.2$ KO mice following PNL.

**Notes:** (**A**) The distribution of cap$^+$ and cap$^-$ cells (**a**) as well as the capsaicin current amplitude (**b**) of cap$^+$ cells was similar in WT and PNL $Ca_v3.2$ KO mice. (**B**–**F**) T-type $Ca^{2+}$ currents were measured via two different methods as described before (see Fig. 2). (**B**–**D**) Standard protocol. (**B**) Representative total $Ca^{2+}$ current traces of a cap$^+$ $Ca_v3.2$ KO sham (**a**) and a cap$^+$ $Ca_v3.2$ KO PNL cell (**b**) elicited by a standard protocol. (**C**) The amplitude of the total $Ca^{2+}$ current at any given potential was measured from the end of the pulse to its peak and average current–voltage curves were constructed (current–voltage curve shown for cap$^+$ cells). (**D**) Histograms indicating average T-type currents from $Ca_v3.2$ KO sham and $Ca_v3.2$ KO PNL mice at –30 mV. Note the increase of the T-type current in cap$^+$ cells following PNL (**a**), whereas T-type currents were not significantly altered in cap$^-$ cells (**b**). (**E, F**) Preconditioning pulse. (**E**) Total $Ca^{2+}$ currents were measured by a depolarizing pulse to –30 mV (**a**). (**b**) and (**c**) depict representative current traces of a cap$^+$ $Ca_v3.2$ KO sham and a cap$^+$ $Ca_v3.2$ KO PNL cell, respectively. (**d**) The same pulse protocol with the addition of a preconditioning pulse to –40 mV was applied to inactivate all T-type currents and the resulting HVA current was measured. Representative current traces of a cap$^+$ $Ca_v3.2$ KO sham (**e**) and a cap$^+$ $Ca_v3.2$ KO PNL cell (**f**) are shown. The T-type current was obtained by digitally subtracting the HVA current component from the total $Ca^{2+}$ current. Representative current examples of a cap$^+$ $Ca_v3.2$ KO sham (**g**) and a cap$^+$ $Ca_v3.2$ KO PNL cell (**h**). (**F**) As for WT mice, peak T-type currents were significantly increased in cap$^+$ $Ca_v3.2$ KO cells following PNL (**a**), whereas there was no significant alteration for cap$^-$ cells (**b**). *$P \leq 0.05$

**Abbreviations:** DRG, dorsal root ganglion; HVA, high voltage activated; KO, knockout; PNL, partial sciatic nerve ligation; WT, wild type.

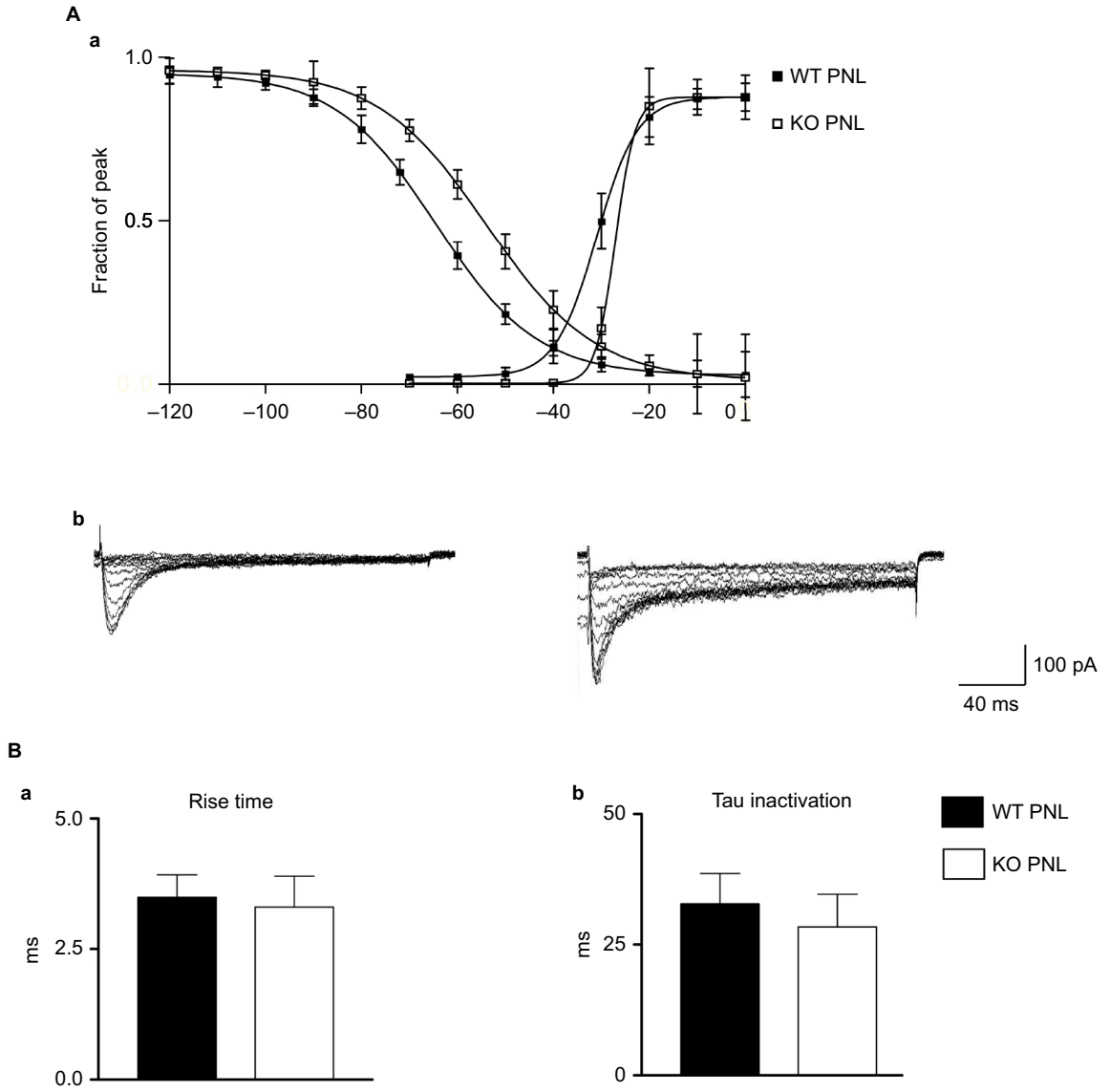


**Figure 6** T-type current characteristics are not different between cap$^+$ cells of PNL WT and PNL $Ca_v3.2$ KO mice.

**Notes:** (**A**) (**a**) Steady-state activation and inactivation profiles of T-type currents of cap$^+$ cells from ligated WT and $Ca_v3.2$ KO mice. For analysis of the steady-state voltage-dependent activation behavior, peak currents from individual cells elicited by the standard protocol (Figures 2 and 5) were transformed into chord conductances, normalized, and then fitted with a Boltzmann equation: $y = (\mathbf{A1}–\mathbf{A2})/(1+ e^{(x-V50/dx)})+ A2$, where A1 is the minimum current, A2 the maximum current, V50 the voltage of half-maximal activation, and dx the slope factor. For analysis of the steady-state voltage-dependent inactivation of T-type currents, currents were evoked by test steps to –30 mV after a 500 ms pre-pulse at potentials from –120 mV to 0 mV in 10 mV increments. (**b**) Representative current samples are depicted for a cap$^+$ WT PNL cell (left panel) and a cap$^+$ $Ca_v3.2$ KO PNL cell (right panel). Peak currents were then normalized to the maximum current and fitted with the Boltzmann equation. Boltzmann functions constructed from the average values of V50 and dx are superimposed on the depicted data points. There were no differences in the voltage dependence of cap$^+$ cells from ligated WT and $Ca_v3.2$ KO mice (steady-state activation: the half-maximal conductance V50 was in cap$^+$ WT PNL cells –31.0±3.1 mV with a slope factor dx 4.3±0.5 and in cap$^+$ $Ca_v3.2$ KO PNL cells: –27.1±2.3 mV with a slope factor 2.1±1.0. Steady-state inactivation: the half-maximal availability in cap$^+$ WT PNL cells was at –64.4±2.4 mV with a slope factor –10.5±0.8, for cap$^+$ $Ca_v3.2$ KO PNL cells V50 was –53.0±4.3 mV with a slope factor –11.3±1.8 (for all parameters $P>0.05$). (**B**) Time-dependent activation (10%–90% rise time) (**a**) and time-dependent inactivation time constant (τ) (**b**) (single-exponential fit of the decaying portion of the current wave form) of the T-type current at –30 mV in the standard protocol. No significant differences were found between cap$^+$ WT PNL cells and cap$^+$ $Ca_v3.2$ KO PNL cells (for both $P>0.05$).

**Abbreviations:** KO, knockout; PNL, partial sciatic nerve ligation; WT, wild type.

burst firing. Hyperexcitability of nociceptors is thought to be directly linked to neuropathic pain behavior in vivo.[22,23] Therefore, the increase of the T-type current in capsaicin-responsive neurons seen in our study may be crucially involved in the hyperexcitability of these cells leading to neuropathic pain behavior.

In situ hybridization experiments have shown that $Ca_v3.2$ is the most abundant T-type channel isoform in small- and medium-sized DRG neurons, while $Ca_v3.3$ displays only modest and $Ca_v3.1$ no relevant expression.[24] Consistently, our electrophysiological experiments of WT and $Ca_v3.2$ KO mice showed that the majority of the T-type current in

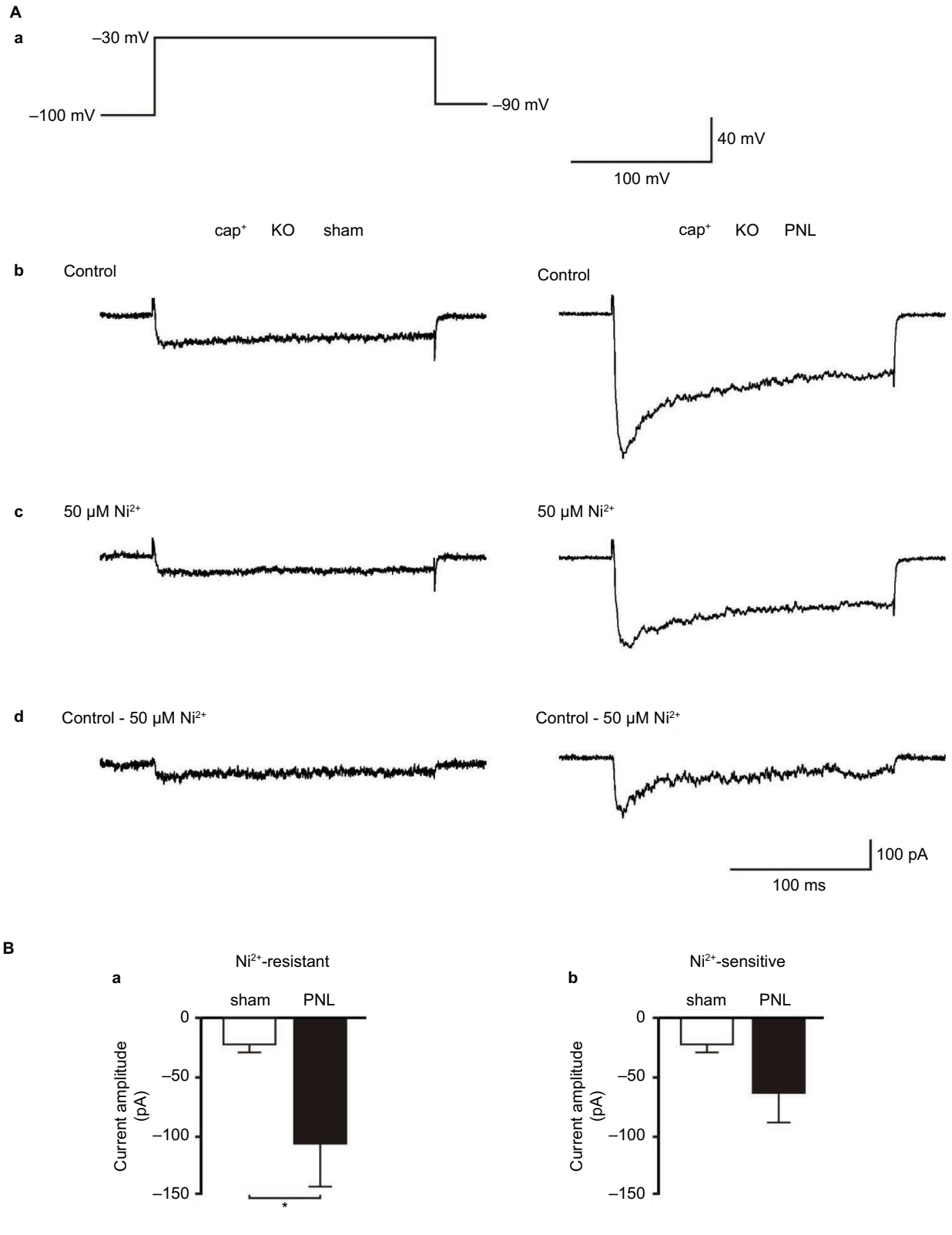


**Figure 7** A $Ni^{2+}$-resistant T-type current component is increased in $cap^+$ cells of $Ca_v3.2$ KO mice following PNL.

**Notes: (A)** Total $Ca^{2+}$ currents were elicited via a standard voltage protocol and the peak T-type $Ca^{2+}$ current was quantified at –30 mV by subtracting the sustained current at the end of the depolarizing pulse from the peak current response (**a**). (**b**) Representative current traces of a $cap^+$ $Ca_v3.2$ KO sham (left) and a $cap^+$ $Ca_v3.2$ KO PNL cell (right). (**c**) By application of 50 µM $Ni^{2+}$, a $Ni^{2+}$-resistant current component was isolated (left: $cap^+$ $Ca_v3.2$ KO sham, right: $cap^+$ $Ca_v3.2$ KO PNL). (**d**) The $Ni^{2+}$-sensitive component was obtained by digitally subtracting the $Ni^{2+}$-resistant component from the total $Ca^{2+}$ current (left: $cap^+$ $Ca_v3.2$ KO sham, right: $cap^+$ $Ca_v3.2$ KO PNL). (**B**) The average peak current amplitude of the $Ni^{2+}$-resistant current of $cap^+$ $Ca_v3.2$ KO cells is increased following PNL compared to sham-operated animals (**a**), whereas the $Ni^{2+}$-sensitive current is not significantly altered (**b**), *P≤0.05.

**Abbreviations:** KO, knockout; PNL, partial sciatic nerve ligation.

small cap$^+$ DRG neurons is mediated by the $Ni^{2+}$-sensitive $Ca_v3.2$ subunit. However, these experiments revealed further that the PNL-induced increase of the T-type current in cap$^+$ DRG neurons is not caused by the predominant $Ni^{2+}$-sensitive $Ca_v3.2$ component but is rather due to the $Ni^{2+}$-resistant T-type current component. According to this, PNL of $Ca_v3.2$ KO mice led to mechanical allodynia indistinguishable to that of ligated WT mice, ruling out a relevant role of $Ca_v3.2$ in PNL-induced neuropathic pain.

Consistent with our data, a previous in vivo study showed that gene KO of $Ca_v3.2$ did not prevent the development of thermal and mechanical hyperalgesia following spinal nerve ligation.[10] However, there are other studies suggesting a pronociceptive role of $Ca_v3.2$ in neuropathic pain. For example, in an animal model of painful diabetic polyneuropathy, molecular knockdown of $Ca_v3.2$ by intrathecally injected antisense oligodeoxynucleotides reversed both neuropathic pain behavior and upregulation of the T-type $Ca^{2+}$ current in small-sized neurons.[5] Bourinet et al showed that intrathecal administration of $Ca_v3.2$ antisense oligodeoxynucleotides induced a large reduction of T-type currents in DRG neurons and reversed neuropathic pain behavior in rats with chronic constriction injury.[8] However, a reduction of T-type currents in DRG neurons of neuropathic pain animals was not reported. These discrepancies could be caused by differences in the type of pain model or species used. Alternatively, discrepancies may be due to differences between null KO by gene targeting and region-specific knockdown with antisense oligonucleotides. For example, Bourinet et al showed that the antisense treatment directed toward $Ca_v3.2$ did not influence the mRNA levels of the other $Ca_V3$ genes, but it cannot be excluded that there are other unknown off-target effects. In addition, the antisense treatment directed against $Ca_v3.2$ induced only a 42% reduction of the mRNA level of this channel subunit within the lumbar DRGs.[8] Thus, in contrast to the KO approach of our experiments, where the $Ca_v3.2$ gene expression is completely lacking, a 100% knockdown cannot be achieved with antisense treatment.[11]

On the other hand, it is also possible that compensatory mechanisms might have eliminated the need for $Ca_v3.2$ in $Ca_v3.2$ KO mice. However, this seems to be unlikely, since in untreated/sham-operated $Ca_v3.2$ KO mice, the T-type $Ca^{2+}$ current was very small without signs of a compensatory increment of the $Ni^{2+}$-resistant T-type current components. In addition, the PNL-induced increase of the $Ni^{2+}$-resistant T-type current in WT mice was identically found in KO mice, making a KO-specific compensatory increment after PNL unlikely. However, a compensatory upregulation of other current components cannot be totally excluded in the KO condition.

Altogether, our results suggest a pronociceptive role of $Ca_v3.1$ and/or $Ca_v3.3$ in the PNL model of neuropathic pain. Consistently, it has been shown that neuropathic pain due to $L_5$ spinal nerve ligation (SNL) was reduced in $Ca_v3.1$ KO mice and that intrathecal administration of $Ca_v3.3$ antisense oligonucleotides reversed neuropathic pain behavior in rats following chronic compression of DRGs.[9,25] However, an electrophysiological characterization of T-type $Ca^{2+}$ currents in these animal models is missing.

## Conclusion

In summary, our results revealed an upregulation of T-type currents in capsaicin-responsive, small DRG neurons following partial ligation of the sciatic nerve. This upregulation is not due to the predominantly expressed $Ca_v3.2$ subunit, but rather caused by a $Ni^{2+}$-resistant current. As T-type currents are critically involved in enhancing neuronal excitability and hyperexcitability of nociceptors is directly associated to neuropathic pain behavior, blocking of peripheral T-type channels may offer new therapeutic options for the treatment of neuropathic pain. The finding that $Ca_v3.2$ is not critically involved in the pathology, at least in the PNL model, may be important for the development of target-specific drugs. Further studies using, for example, KO/knockdown animals of the $Ni^{2+}$-resistant $Ca_v3.1$ or $Ca_v3.3$ channels are needed for more information about the involved subunit.

## Acknowledgments

This work was supported by the BONFOR Program of the University of Bonn, Germany. We thank Susanne Schoch, University of Bonn Medical Center, Germany, for providing $Ca_v3.2$ KO mice. We thank Olivia Steffan and Lioba Dammer for excellent technical assistance. We thank Katlynn Carter for critically reading the manuscript.

## Disclosure

The authors report no conflicts of interest in this work.

## References

1. Perez-Reyes E. Molecular physiology of low-voltage-activated t-type calcium channels. *Physiol Rev*. 2003;83(1):117–161.
2. Jagodic MM, Pathirathna S, Nelson MT, et al. Cell-specific alterations of T-type calcium current in painful diabetic neuropathy enhance excitability of sensory neurons. *J Neurosci*. 2007;27(12):3305–3316.
3. Jagodic MM, Pathirathna S, Joksovic PM, et al. Upregulation of the T-type calcium current in small rat sensory neurons after chronic constrictive injury of the sciatic nerve. *J Neurophysiol*. 2008;99(6):3151–3156.

4. Latham JR, Pathirathna S, Jagodic MM, et al. Selective T-type calcium channel blockade alleviates hyperalgesia in ob/ob mice. *Diabetes*. 2009;58(11):2656–2665.
5. Messinger RB, Naik AK, Jagodic MM, et al. In vivo silencing of the $Ca_{(V)}3.2$ T-type calcium channels in sensory neurons alleviates hyperalgesia in rats with streptozocin-induced diabetic neuropathy. *Pain*. 2009;145(1–2):184–195.
6. Yue J, Liu L, Liu Z, Shu B, Zhang Y. Upregulation of T-type $Ca^{2+}$ channels in primary sensory neurons in spinal nerve injury. *Spine*. 2013;38(6):463–470.
7. McCallum JB, Kwok WM, Mynlieff M, Bosnjak ZJ, Hogan QH. Loss of T-type calcium current in sensory neurons of rats with neuropathic pain. *Anesthesiology*. 2003;98(1):209–216.
8. Bourinet E, Alloui A, Monteil A, et al. Silencing of the Cav3.2 T-type calcium channel gene in sensory neurons demonstrates its major role in nociception. *Embo J*. 2005;24(2):315–324.
9. Wen XJ, Li ZJ, Chen ZX, et al. Intrathecal administration of Cav3.2 and Cav3.3 antisense oligonucleotide reverses tactile allodynia and thermal hyperalgesia in rats following chronic compression of dorsal root of ganglion. *Acta Pharmacol Sin*. 2006;27(12):1547–1552.
10. Choi S, Na HS, Kim J, et al. Attenuated pain responses in mice lacking $Ca_{(V)}3.2$ T-type channels. *Genes Brain Behav*. 2007;6(5):425–431.
11. Chen CC, Lamping KG, Nuno DW, et al. Abnormal coronary function in mice deficient in alpha1H T-type $Ca^{2+}$ channels. *Science*. 2003;302(5649):1416–1418.
12. Malmberg AB, Basbaum AI. Partial sciatic nerve injury in the mouse as a model of neuropathic pain: behavioral and neuroanatomical correlates. *Pain*. 1998;76(1–2):215–222.
13. Harper AA, Lawson SN. Conduction velocity is related to morphological cell type in rat dorsal root ganglion neurones. *J Physiol*. 1985;359:31–46.
14. Rigaud M, Gemes G, Barabas ME, et al. Species and strain differences in rodent sciatic nerve anatomy: implications for studies of neuropathic pain. *Pain*. 2008;136(1–2):188–201.
15. Petruska JC, Napaporn J, Johnson RD, Gu JG, Cooper BY. Subclassified acutely dissociated cells of rat DRG: histochemistry and patterns of capsaicin-, proton-, and ATP-activated currents. *J Neurophysiol*. 2000;84(5):2365–2379.
16. Snider WD, McMahon SB. Tackling pain at the source: new ideas about nociceptors. *Neuron*. 1998;20(4):629–632.
17. McCleskey EW, Gold MS. Ion channels of nociception. *Annu Rev Physiol*. 1999;61:835–856.
18. Caterina MJ, Julius D. The vanilloid receptor: a molecular gateway to the pain pathway. *Annu Rev Neurosci*. 2001;24(1):487–517.
19. Lee JH, Gomora JC, Cribbs LL, Perez-Reyes E. Nickel block of three cloned T-type calcium channels: low concentrations selectively block alpha1H. *Biophys J*. 1999;77(6):3034–3042.
20. Abdulla FA, Smith PA. Axotomy- and autotomy-induced changes in $Ca^{2+}$ and K+ channel currents of rat dorsal root ganglion neurons. *J Neurophysiol*. 2001;85(2):644–658.
21. Djouhri L, Bleazard L, Lawson SN. Association of somatic action potential shape with sensory receptive properties in guinea-pig dorsal root ganglion neurones. *J Physiol*. 1998;513(Pt 3):857–872.
22. Djouhri L, Koutsikou S, Fang X, McMullan S, Lawson SN. Spontaneous pain, both neuropathic and inflammatory, is related to frequency of spontaneous firing in intact C-fiber nociceptors. *J Neurosci*. 2006;26(4):1281–1292.
23. Djouhri L, Fang X, Koutsikou S, Lawson SN. Partial nerve injury induces electrophysiological changes in conducting (uninjured) nociceptive and nonnociceptive DRG neurons: Possible relationships to aspects of peripheral neuropathic pain and paresthesias. *Pain*. 2012;153(9):1824–1836.
24. Talley EM, Cribbs LL, Lee JH, Daud A, Perez-Reyes E, Bayliss DA. Differential distribution of three members of a gene family encoding low voltage-activated (T-type) calcium channels. *J Neurosci*. 1999;19(6):1895–1911.
25. Na HS, Choi S, Kim J, Park J, Shin HS. Attenuated neuropathic pain in Cav3.1 null mice. *Mol Cells*. 2008;25(2):242–246.